

Rapid Raman Spectroscopy of Musculoskeletal Tissue using a Visible Laser and an Electron-Multiplying CCD (EMCCD) Detector

Kurtulus Golcuk^a, Gurjit S. Mandair^a, Andrew F. Callender^a, William F. Finney^a, Nadder Sahar^b, David H. Kohn^{b,c} and Michael D. Morris^{*a}

^aDepartment of Chemistry, University of Michigan, Ann Arbor, MI, 48109

^bDepartment of Biologic and Materials Sciences, University of Michigan, Ann Arbor, MI 48109

^cDepartment of Biomedical Engineering, University of Michigan, Ann Arbor, MI 48109

ABSTRACT

Background fluorescence can often complicate the use of Raman microspectroscopy in the study of musculoskeletal tissues. Such fluorescence interferences are undesirable as the Raman spectra of matrix and mineral phases can be used to differentiate between normal and pathological or microdamaged bone. Photobleaching with the excitation laser provides a non-invasive method for reducing background fluorescence, enabling 532 nm Raman hyperspectral imaging of bone tissue. The signal acquisition time for a 400 point Raman line image is reduced to 1-4 seconds using electron-multiplying CCD (EMCCD) detector, enabling acquisition of Raman images in less than 10 minutes. Rapid photobleaching depends upon multiple scattering effects in the tissue specimen and is applicable to some, but not all experimental situations.

Keywords: Raman microspectroscopy, Fluorescence, Photobleaching, Bone, Raman photon migration, EMCCD

1. INTRODUCTION

Raman microspectroscopy and Raman imaging are increasingly becoming widely used tools for the study of bone tissue. Our own group has used Raman spectroscopic methodology to examine biomechanical properties of bone tissue [1-5] and the mineralization process itself [6]. As in other fields, Raman microspectroscopy and Raman imaging of bone tissue offer in a single set of measurements both high chemical composition and physical property information along with micron-range spatial resolution. Using multivariate curve resolution techniques, small variations in local composition or physical properties can be detected and imaged [1-3].

While Raman spectroscopy is a useful bone tissue imaging method, it has two widely acknowledged limitations. Because the tissue is fluorescent, Raman spectroscopy and imaging are frequently performed with a near-infrared (NIR) laser, such as a 785 nm diode laser, which excites little bone fluorescence. Compared to the green (532 nm) lasers widely used in Raman spectroscopy, the use of a deep red or near-infrared laser results in relatively long acquisition times. We routinely collect a line of 128 or 256 spectra in 30 sec to 3 min using a line focused 785 nm laser. The long acquisition time is a result of the unfavorable dependence of Raman intensity with excitation wavelength and the low quantum efficiency of CCD detectors at wavelengths above about 800 nm. At 785 nm, Raman scattering is about five times less intense than at 532 nm and the quantum efficiency of a deep depletion back-illuminated CCD – currently the best available detector for the 800-900 nm range in which 785 nm excited bone mineral spectra and matrix amide I and amide III spectra are found – is about 30-40% [7]. By contrast, a back-illuminated CCD operating in the 550-600 nm range has quantum efficiency about 80-90%.

In addition, bone scatters light. Since the pioneering study of Matousek et al. [8] using time-resolved Raman spectroscopy, the effects of multiple scattering on Raman spectra have been intensively investigated [9, 10]. It is known that as light propagates through a scattering medium such as bone [11-13], the light beam spreads out, resulting in

*Corresponding author. Email: mdmorris@umich.edu; Tel: +1 734-764-7560; Fax: +1 734-649-1179

Raman occurring at sites removed from the initial direction of laser beam entry into the tissue. The Raman scattered light itself undergoes multiple scattering. The overall effect can be modeled using Monte Carlo simulations. The effects of multiple scattering are now generally called Raman photon migration [14], by analogy to multiple scattering effects in absorption and fluorescence spectroscopy.

The recently developed electron-multiplied CCD (EMCCD) [15] provides low noise gain and has the potential for dramatic reductions in Raman spectral acquisition times. The back-illuminated EMCCD has already been applied to low-light level fluorescence imaging applications, including ultra-sensitive detection of intracellular calcium concentrations [15], optical tracking of single proteins [16] and imaging of tumor-targeted molecular probes [17]. We have reported acquisition times as short as 0.01 sec [18].

To fully exploit the sensitivity of the back-illuminated EMCCD for 532 nm laser Raman imaging of bone, it is necessary to reduce the fluorescence background, which otherwise overwhelms the Raman bone spectrum. We have previously shown that photochemical bleaching with a 532 nm laser [19] is a simple and effective method for reducing the fluorescence background. However, our previous protocol required a four hour treatment time. In this study, we investigate the effects of photon migration on fluorescence removal by photochemical bleaching. We show that in some cases fluorescence background reduction occurs within a few minutes, after which rapid Raman imaging is possible. Raman photon migration affects the bleaching time and can be used to shorten the overall measurement time.

2. MATERIALS AND METHODS

The hyperspectral Raman imaging system is similar to our earlier design [20], except that a scanning stage that translates the specimen under a fixed laser line has been replaced by a galvanometer scanning mirror that sweeps the laser line across the stationary specimen. It consists of a research grade microscope (ME600L, Nikon USA), a 2 W 532 nm laser (Millennia II, Spectra Physics, Mountain View, CA), and an $f/1.8$ axial transmissive spectrograph (HoloSpec, Kaiser Optical Systems, Inc., Ann Arbor, MI). An infinity corrected $10\times/0.45$ NA plan achromat objective (Nikon) was used for focusing the 532 nm laser line onto the specimen and for collecting the Raman scatter. The detector is a 512×512 pixel back-illuminated EMCCD (iXON, Andor Technology, Belfast, Northern Ireland.) operated at full gain. A uniform laser line was generated using a 5° Powell lens (StockerYale Canada, Montreal, PQ) [21]. Hyperspectral images are built up by scanning the line-focused laser across the specimen [22] using a single axis scanning mirror (6240H, Cambridge Technology, Inc., Cambridge, MA). The mirror can be positioned to approximately $\pm 0.2 \mu\text{m}$ with a settling time 1-3 millisecond. Mirror and camera control and data acquisition are performed as a LabVIEW (National Instruments, Austin, TX) VI program.

The spectrograph was calibrated against an Ar emission lamp. Spectral data analysis was performed with Matlab (Math Works, Inc.) or in GRAMS/32 (Galactic Industries). Prior to data analysis, all spectral data were processed with removal of the curvature of the spectral bands caused by the large gathering angle of the spectrograph, subtraction of dark current and removal of noise spikes. The spectra were analyzed using principal components analysis to identify spectral factors followed by band-target entropy minimization (BTEM) [23] extract the spectra and generate score plot images.

Bovine bone specimens obtained from a local abattoir were sectioned into $5 \times 2 \times 10$ mm blocks under constant irrigation using a diamond wheel saw (South Bay Technology, Inc., San Clemente, CA). The specimens were wrapped in calcium-buffered saline (CBS) soaked gauze, and frozen (-30°C) until required. Two different photobleaching protocols were examined. In protocol 1 a bone specimen was removed from CBS solution, allowed to dry superficially and photobleached for 10 sec – 3 min prior to Raman data acquisition. In protocol 2 the specimen was kept moist by suspension in a chamber with a cover containing an opening just large enough to accommodate a microscope objective [4]. High humidity was maintained by a thin layer of water in the bottom of the chamber. Just prior to an experiment, a bone specimen was briefly immersed in deionized water to establish hydration and then photobleached for 2-20 min prior to Raman data acquisition.

Following photochemical bleaching, Raman imaging was performed. A series of 50-100 transects, was taken with 1.0 μm steps, using laser power of 100 mW at the objective with an integration time was 4 sec per line. In each case the specimen was photobleached with line illumination only at one end of the scanned region.

For comparison to results obtained with fresh tissue, an archived specimen of bone tissue that had previously been embedded in polymethyl methacrylate (PMMA) and sectioned for microscopy was examined. Pretreatment according to protocol 1 was employed on this specimen. Raman imaging with 4 sec/frame acquisitions was used to generate a 50 line image of a region of this specimen.

3. RESULTS AND DISCUSSION

Figure 1 shows the percentage decay of fluorescence background for superficially dry and hydrated specimens. From Figure 1 it is clear that the rate of photochemical bleaching of hydrated and dried specimens is dramatically different. While the exact photobleaching time varies between specimens, the patterns are the same in every case.

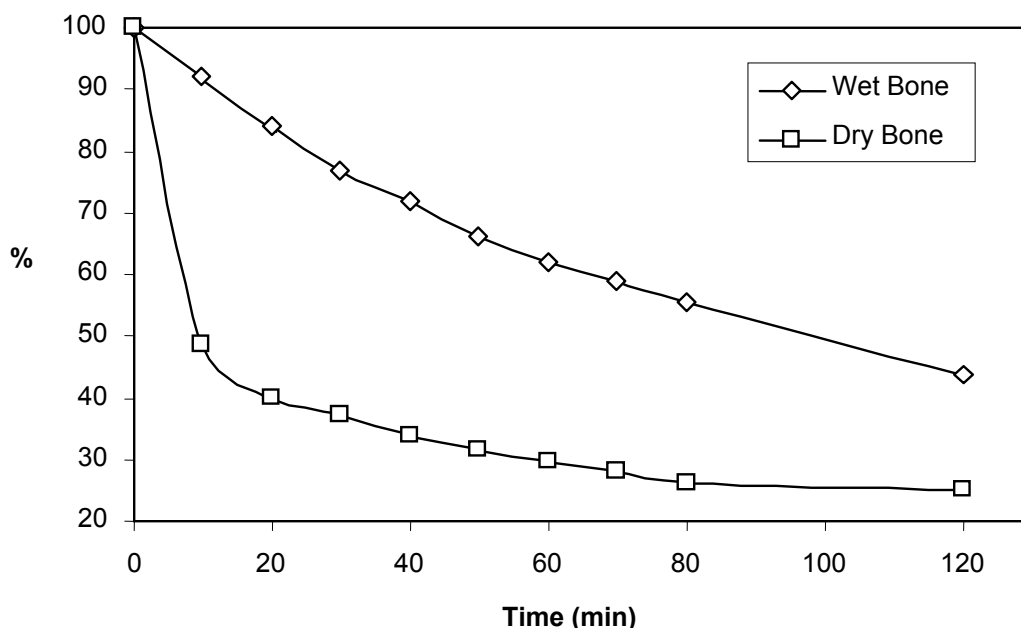


Figure 1. Time dependence of fluorescence background reduction for wet and dry bone. 100 mW laser power at the specimen.

At the beginning of an experiment most of the Raman bands are observed on a high fluorescence background. In many cases, only the intense phosphate ν_1 (ca. 957 cm^{-1}) band is easily seen above the background. However, photobleaching occurs rapidly. Figure 1 shows a typical background decay for bone that has been photobleached according to protocol 1. After about 10 minutes, the fluorescence background is reduced to less than 50% of the initial value. Further decrease occurs over time, but the rate is much lower. The decay is more rapid if the laser power is increased. The photobleaching rate is greatly reduced if the bone is immersed in water or buffer, as shown in the figure. For the specimen of figure 1, prebleaching the fully hydrated tissue immersed in water or buffer for 10 minutes results in only a 5% reduction in fluorescence. In other hydrated specimens the intensity reduction was between 5% and 10%. To establish that rapid photobleaching is not limited to fresh tissue, we performed a similar experiment on an archived bone specimen that had been embedded in PMMA. As with the fresh, dried tissue, rapid fluorescence reduction was observed (not shown).

Figure 2 shows reflected light (frame 2a), fluorescence (frame 2b) and Raman images (frames 2c and 2d) of a section of cortical bone. A single 15 minute prebleach has been performed at the left edge of the scanned region. The line scan direction is left to right. Following the prebleach, the Raman image has been obtained with a 4 sec/line acquisition. There has been no prebleaching of the specimen except at left edge of the imaged region. The features are similar in each image, except that the two mineral component Raman images show different spatial dependences (Figures 2c and 2d).

We have measured the areas of the major phosphate and carbonate bands and the areas of the matrix collagen bands that are within the field of view of the spectrograph/CCD. We find that band intensities and band areas are independent of photobleaching time for at least 30 minutes. This negative finding cannot be interpreted as meaning that there is no photodegradation of bone matrix, but only that if there is any damage; the extent is too small to be spectroscopically detectable.

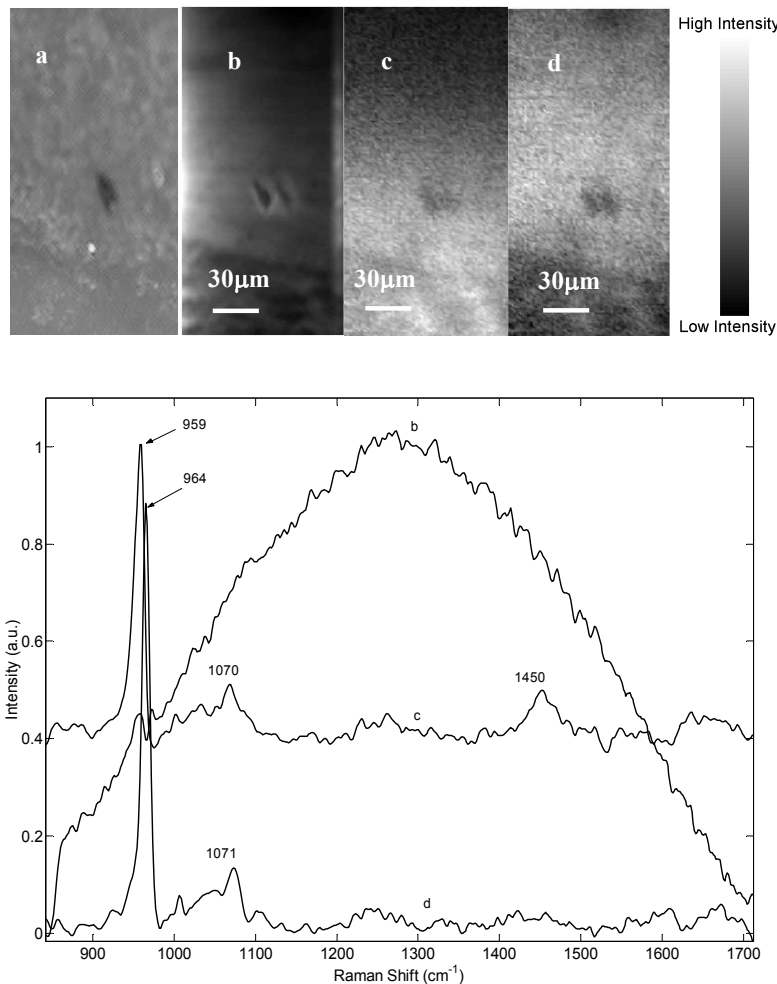


Figure 2. Reflected light (a), fluorescence (b) and Raman images (c and d) of a section of cortical bone, and corresponding Raman spectra of Raman images. Raman images are $296\mu\text{m} \times 107\mu\text{m}$ with $2\mu\text{m}$ resolution.

The surprising effect is that the fluorescence background is almost constant across the entire Raman image, even though the image is 100 scans wide. The time to position the galvo mirror was no more than 3 millisecc and the time to transfer a

frame of data from camera to computer is 50 millisecond. The image is collected with a total time of about 4.053 sec/line, or about 405 sec total. This time is less than half the 900 sec (15 minutes) prebleaching time.

We attempted to repeat the same procedure with fully hydrated and immersed specimens, but were unsuccessful. With specimens kept moistened, the fluorescence background did not decrease rapidly (Figure 1) and it was necessary to prebleach at each line prior to acquisition of Raman spectra.

The transfer of photobleaching is not limited to fresh tissue. We repeated the imaging experiments using archived murine tissue embedded in PMMA. As with the fresh tissue, a 15 minute prebleach was applied at one end of the region to be imaged. A bone tissue image obtained by this method is shown as Figure 3. In this figure the Raman image is overlaid on a reflected light image. The overlay illustrates the fidelity of the spectroscopic image obtained on a type of specimen traditionally assumed to be limited by intense fluorescence. As with fresh tissue, the background reduction was greater than 50%, and the background did not change much during the 200 sec (50 frames) acquisition time.

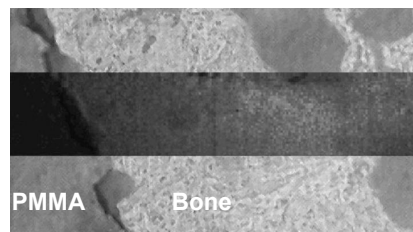


Figure 3. Reflected light and Raman images of murine femoral bone.

The Raman imaged area (dark) is overlaid on the corresponding reflected light image, illustrating the fidelity of the spectroscopic image.

We attribute the global effectiveness of photochemical bleaching at a single line to photon migration. Although photons are injected in a line along one side of the region to be imaged, scattering causes them to diffuse across the entire field of view, and even further. The propagation time is a few tens of picoseconds and the attenuation over the 50-100 μm region is small enough that photobleaching efficiency is nearly constant. If the tissue is dry, it is not necessary to prebleach at every point to be imaged.

4. CONCLUSIONS

In most imaging applications photon migration is a complication that reduces image contrast and resolution. Our Raman imaging system uses the spectrograph as a spatial filter. As a consequence, high resolution images are obtained, without the blurring sometimes found with widefield Raman imaging microscopy. Just as importantly in this case, photon migration can be used to reduce prebleaching time to a surprisingly short duration, because it is not necessary to directly illuminate the entire region of interest. Photon migration enables use of the low noise and high frame rate properties of the EMCCD to perform rapid Raman imaging. Although we have used low laser power for these experiments, there is no reason that increased laser power can not be used to decrease acquisition time even further.

The methodology is not completely general. It is easily applicable to fresh or archived specimens, provided that they have not been treated with histological stains that absorb at the laser wavelength. If maintenance of complete hydration is important, as in Raman biomechanical studies of bone [5], rapid single line photobleaching prior to imaging cannot be recommended at this point.

ACKNOWLEDGEMENTS

This work has been supported by NIH grant R01 AR052010 to M.D.M.

REFERENCES

1. J. A. Timlin, A. Carden, M. D. Morris, R. M. Rajachar, D. H. Kohn, Raman spectroscopic imaging markers for fatigue-related microdamage in bovine bone, *Anal. Chem.*, 72 (2000) 2229-2236.
2. M. D. Morris, A. Carden, R. M. Rajachar, D. H. Kohn, Effects of applied load on bone tissue as observed by Raman spectroscopy, *Proc SPIE* 4614 (2002) 47-54.
3. A. Carden, R. M. Rajachar, M. D. Morris, D. H. Kohn, Ultrastructural changes accompanying the mechanical deformation of bone tissue: A Raman imaging study, *Calcif. Tissue Int.*, 72(2003) 166-175.
4. M. D. Morris, W. F. Finney, R. M. Rajachar, D. H. Kohn, Bone tissue ultrastructural response to elastic deformation probed by Raman spectroscopy, *Faraday discuss.*, 126 (2004) 159-168.
5. A. C. Callender, W. F. Finney, M. D. Morris, N. D. Sahar, D. H. Kohn, K. M. Kozloff, S. A. Goldstein, Dynamic mechanical testing system for Raman microscopy of bone tissue specimens, *Vib. Spectrosc.*, 38 (2005) 101-105.
6. A. Stewart, D.A. Shea, C. p. Tarnowski, M.D. Morris, D. Wang, R. Franceschi, D. L. Lin and E. Keller, Trends in early mineralization of murine calvarial osteoblastic cultures: a Raman microscopic study, *J. Raman Spectrosc.* 33 (2002) 536-543.
7. J. R. Janesick, Scientific charge coupled devices, SPIE press, USA, 2001.
8. P. Matousek, I. P. Clark, E.R.C. Draper, M. D. Morris, A.E. Goodship, N. Everall, M. Towrie, W. F. Finney, A.W. Parker, Subsurface Probing in Diffusely Scattering Media Using Spatially Offset Raman Spectroscopy, *Appl. Spectrosc.* 59 (2005) 393-400.
9. N. Everall, T. Hahn, P. Matousek, A.W. Parker, M. Towrie, Photon Migration in Raman Spectroscopy, *Appl. Spectrosc.* 58 (2004) 591-597.
10. N. Everall, T. Hahn, P. Matousek, A.W. Parker, M. Towrie, Picosecond Time-Resolved Raman Spectroscopy of Solids: Capabilities and Limitations for Fluorescence Rejection and the Influence of Diffuse Reflectance, *Appl. Spectrosc.* 55 (2001) 1701-1708.
11. M. D. Morris, A.E. Goodship, E.R.C. Draper, P. Matousek, M. Towrie, A.W. Parker, Kerr-gated picosecond Raman spectroscopy and Raman photon migration of equine bone tissue with 400-nm excitation, *Proc. SPIE*, 5321 (2004) 164-169.
12. M. D. Morris, P. Matousek, M. Towrie, A. W. Parker, A. E. Goodship, E.R.C. Draper, Kerr-gated time-resolved Raman spectroscopy of equine cortical bone tissue *J. Biomed. Opt.* 10 (2005) 014014.
13. E. R. C. Draper, M. D. Morris, N. P. Camacho, P. Matousek, M. Towrie, A. W. Parker, A. E. Goodship, Novel Assessment of Bone Using Time-Resolved Transcutaneous Raman Spectroscopy; *J. Bone and Min. Research*, 20 (2005) 1968-1972.
14. M. V. Schulmerich, W. F. Finney, R. A. Fredericks, and M. D. Morris, Subsurface Raman spectroscopy and mapping using a globally illuminated non-confocal fiber optic array probe in the presence of Raman photon migration. *Appl. Spectrosc.* In press.
15. C. G. Coates, D. J. Denvir, N. G. Mchale, K. D. Thornbury, M. A. Hollywood, Optimizing low-light microscopy with back-illuminated electron multiplying charge-coupled device: enhanced sensitivity, speed, and resolution, *J. Biomed. Opt.* 9 (2004) 1244-1252.
16. A. Sarkar, R. B. Robertson, J. M. Fernandez, Simultaneous atomic force microscopy and fluorescence measurements of protein unfolding using a calibrated evanescent wave, *PNAS*, 101 (2004) 12882-12886.
17. S. V. Patwardhan, S. R. Bloch, S. Achilefu, J. P. Culver, Time-dependent whole-body fluorescence tomography of probe bio-distributions in mice, *Opt. Express*, 13 (2005) 2564-2577.
18. M. Tripathi, W. F. Finney, M. D. Morris, T. Chen, K. Golcuk, Rapid Raman microspectroscopy and imaging: The role of the electron multiplied CCD (EMCCD), Federation of Analytical Chemistry and Spectroscopy Societies, paper 473, Quebec City, Canada, 2005.
19. D. A. Shea, M. D. Morris, Bone tissue fluorescence reduction for visible laser Raman spectroscopy, *Appl. Spectrosc.*, 56 (2002) 182-186.

20. K. A. Christensen, M. D. Morris, Hyperspectral Raman microscopic imaging using Powell lens line illumination, *Applied Spectroscopy* 52 (1998) 1145-1147.
21. A. Bewsher, I. Powell, and W. Boland, Design of single element laser beam shape projectors, *Applied Optics* 35 (1996) 1654-1958.
22. P.J. Treado and M. D. Morris, Infrared and Raman Spectroscopic imaging, in: M.D. Morris (Ed), *Spectroscopic Imaging of the Chemical State*, Dekker, New York, 1993.
23. E. Widjaja, N. Crane, TC. Chen, M.D. Morris M.A. Ignelzi, B.R. McCreadie, Band-Target Entropy Minimization (BTEM) Applied to Hyperspectral Raman Image Data, *Appl. Spectrosc.* 57 (2003) 1353-1362.